

PACS numbers: 42.65.Jx; 42.65.Re; 52.50.Jm
DOI: 10.1070/QE2012v042n02ABEH014751

Interaction of noncollinear femtosecond laser filaments in sapphire

A.A. Dergachev, V.N. Kadan, S.A. Shlenov

Abstract. **The interaction of two coherent femtosecond laser pulses, propagating at a small angle with respect to each other in a sapphire crystal in the filamentation regime, has been investigated numerically and experimentally. Distributions of the fluence and free-electron density in the laser-plasma channels formed in the crystal are obtained. Additional filaments are found to form outside the plane of initial pulse propagation.**

Keywords: *filamentation, femtosecond radiation, laser plasma, filament interaction.*

1. Introduction

When femtosecond laser radiation propagates in transparent insulators, the light field is self-trapped into a narrow extended structure, referred to as a filament [1, 2]. Filaments are observed in the transverse beam cross section in the form of 'hot points' with a high fluence. The high radiation intensity in a filament leads to photoionisation of the medium and formation of a plasma channel. Unique properties of filaments open radically new possibilities for femtosecond laser technologies in atmospheric optics, microoptics, and other applications [3]. Filamentation is due to the dynamic balance between the Kerr nonlinearity (which leads to self-focusing of the radiation) and defocusing plasma nonlinearity [4]. A filament is formed when the laser pulse peak power exceeds the critical self-focusing power in the medium, P_{cr}. If the peak power exceeds several times the critical value, one plasma channel is formed along the pulse propagation direction. Few percent of the total pulse energy falls on this channel. The rest energy forms a energy reservoir to compensate for the loss in the filament [5]. If the peak pulse power exceeds significantly P_{cr}, the modulation instability [6] leads to the formation of many filaments in the transverse beam cross section, which interact in a complex way; in other words, multiple filamentation develops. The multiple filamentation regime is of special interest in view of studying the propagation of radiation generated in modern high-power laser systems [7]. Here, the interaction between filaments affects significantly the distribution of a high fluence in space. Since the spatial and temporal dynamics of multiple filaments is rather complicated, the problem of determining the fundamental features of interaction between individual filaments is very important.

In the experiments carried out in [8], a beam with a peak power of $25P_{cr}$ was separated in air (in the transverse cross section) into two substructures, which merged then into a unified filament. Two parallel or weakly noncollinear filaments, formed by radiation at different wavelengths, may exchange energy, as a result of which a supplementary filament at another wavelength can be used to compensate for the energy loss in the main filament. A number of researchers [9–11] considered such tools as the time delay between pulses and additional phase modulation (chirp) to control these process.

The detailed experimental study of the filament interaction in air is hindered by the necessity of using high radiation powers (more than 10 GW) and long paths (several tens and hundreds of meters). Using a condensed medium, one can perform experiments under laboratory conditions using relatively low-power sources.

The interaction of two coherent femtosecond laser pulses, propagating at a small angle with respect to each other in a sapphire crystal, was considered in [12]. It was found that interaction of two identical pulses with a peak power of about 10 MW leads to the formation of a unified filament. The character of filamentation was determined by the interference pattern formed in the beam overlap region and depended on the number of fringes within which the radiation peak power exceeded the critical value. In this experiment the energy distribution in space was controlled by changing the phase difference between the light fields of pulses. Light fields with zero phase difference (in-phase pulses) and a phase shift equal to π (out-of-phase pulses) formed, respectively, attracting and repulsing filaments.

Numerically, the problem of interaction of two femtosecond beams with parallel or slightly converging (at a small angle θ) directions, propagating in air, was considered in [13, 14]. It was shown that the spatial energy distribution depends on the phase relation between the light fields of pulses and the angle between their propagation directions. At a small angle θ (0.02°), in-phase pulses tended to form a unified filament, whereas in the out-of-phase case they formed two diverging filaments. If the angle between the beams was 0.2°, they passed through each other to form an interference pattern in the overlap region. Kandidov et al. [15] explained the character of interaction between parallel filaments by the competition for the common energy reservoir. Using numerical simulation, it was shown that, at a relatively low power

A.A. Dergachev, S.A. Shlenov Department of Physics, M.V. Lomonosov Moscow State University, Vorob'evy Gory, 119991 Moscow, Russia; International Laser Center, M.V. Lomonosov Moscow State University, Vorob'evy Gory, 119991 Moscow, Russia; e-mail: dergachev88@yandex.ru, shlenov@physics.msu.ru;
V.N. Kadan Institute of Physics, National Academy of Sciences of Ukraine, prosp. Nauki 46, 03028 Kiev, Ukraine

Received 19 October 2011; revision received 5 December 2011
Kvantovaya Elektronika **42** (2) 125–129 (2012)
Translated by Yu.P. Sin'kov

and small length between the beams, the latter can merge to form a unified filament.

In this study, we investigated experimentally and numerically the distribution of the fluence F and free-electron density upon interaction between two noncollinear focused femtosecond beams in a sapphire crystal. The numerical simulation showed that this interaction leads to the formation of an additional region with a high fluence in the plane oriented perpendicularly to the beam propagation plane. These results are in agreement with the experimental observations, which confirmed the existence of these regions.

2. Schematics of the experimental observation of interaction between filaments in a sapphire crystal

The schematics of the experiment on studying the interaction between two weakly noncollinear pulses in sapphire is shown in Fig. 1. A 120-fs (FWHM) laser pulse with a central wavelength of 818.5 nm passed through an opaque screen with two round holes 1.2 mm in diameter, spaced at a distance of 5 mm. The holes were located symmetrically with respect to the incident beam axis. Two mutually coherent laser beams, propagating in parallel directions in the horizontal oxz plane, were formed behind the screen. Then these pulses, each with a peak power of 26 MW, passed through a collecting lens with a focal length of 35 mm, the geometric focus of which was located inside a sapphire crystal sample at a distance of 0.5 mm from its input face. In this scheme the light fields of both pulses are in-phase. The crystal length was 3 mm and the energy reflection coefficient was 7.6%. The pulse peak power in the sapphire crystal was about 24 MW. The angle between the pulse propagation directions was 4.64°. The beam diameter in the waist was 15 μm in the linear case, and the width of the interference fringes in the overlap region was 10 μm; thus, the beam diameter in the waist covered one fringe and a half.

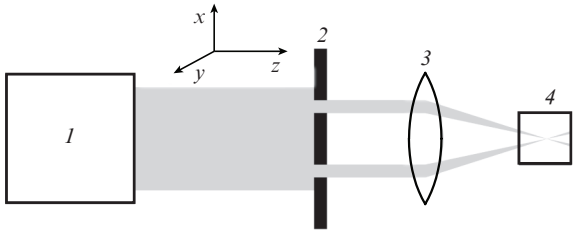

Figure 1. Schematics of the experimental setup (view from above): (*1*) radiation source; (*2*) opaque screen with two round, symmetrically located holes; (*3*) collecting lens; and (*4*) nonlinear medium (sapphire crystal).

The intense luminescence in the region of the beam waist inside the crystal, which arises during filament formation, was recorded through the sample lateral faces using a CCD camera in two mutually perpendicular directions. In one case the camera array was oriented parallel to the horizontal plane oxz (the beam propagation plane) and in the other case it was parallel to the vertical plane oyz (Fig. 1).

The lateral filament luminescence in the visible spectral range, which was experimentally observed, is likely to be due to the recombination of free carriers, which are formed in the regions with a high radiation intensity [12]. In this case, the recorded signal is proportional to the total concentration of free carriers, i.e., the concentration integrated along the observation axis (oy or ox, respectively).

3. Method of numerical analysis

To simulate numerically the propagation of laser radiation in a nonlinear medium, we used a system of equations for a slowly varying complex light field amplitude $A(x, y, z, \tau = t - zn_0/c)$ and a free-electron density $n_e(x, y, z, \tau)$:

$$2ik_0\frac{\partial A}{\partial z} = \Delta_\perp A + 2k_0\tilde{D}A + \frac{2k_0^2}{n_0}(\Delta n_K + \Delta n_p)A - ik_0(\alpha + \delta)A,$$

$$\Delta n_K = n_2 I, \quad I = \frac{cn_0|A|^2}{8\pi}, \quad \Delta n_p = -\frac{\omega_p^2}{2n_0\omega^2}, \quad \omega_p^2 = \frac{4\pi e^2 n_e}{m_e}, \quad (1)$$

$$\frac{\partial n_e}{\partial \tau} = K(|A|^2)(n_e^0 - n_e)\frac{e^2|A|^2\nu_c}{2m_e E_{gap}(\omega_0^2\nu_c^2)}n_e - \frac{n_e}{\tau_{rec}}.$$

Here, $k_0 = 2\pi/\lambda$ is the wave number; n_0 is the refractive index of sapphire; Δn_K and Δn_p are the changes in the refractive index that are due to the Kerr and plasma nonlinearities, respectively; n_2 is the coefficient of cubic nonlinearity (the Kerr response was assumed to be instantaneous); α is the linear attenuation coefficient; δ is the nonlinear absorption coefficient that is related to photoionisation; ω is the pulse carrier frequency; E_{gap} is the sapphire band gap; and τ_{rec} is the carrier recombination time. The operator $\tilde{D}$ describes the dispersion of light in sapphire according to the Sellmeier formula:

$$n^2 - 1 = \frac{A_1\lambda^2}{\lambda^2 - \lambda_1^2} + \frac{A_2\lambda^2}{\lambda^2 - \lambda_2^2} + \frac{A_3\lambda^2}{\lambda^2 - \lambda_3^2}. \quad (2)$$

The coefficients A_i and λ_j were determined in [16]. The photoionisation rate of the medium is described by the function $K(|A|^2)$, which was calculated within the Keldysh model [17]. In addition, the model took into account the avalanche ionisation and recombination of charge carriers.

Numerical simulation was performed using the following values of the parameters for sapphire: $\alpha = 0.081$ cm^{-1}, $n_e^0 = 2.3512 \times 10^{22}$ cm^{-3}, $\nu_c = 10^{14}$ s^{-1}, and $\tau_{rec} = 95$ fs [18]. The Kerr nonlinearity coefficient, according to different data, was in the range $(2.4-3.2) \times 10^{-16}$ cm^2 W^{-1} [19, 20]. The n_2 value was taken to be 2.7×10^{-16} cm^2 W^{-1}, which corresponds to the critical power $P_{cr} = 2$ MW. The sapphire band gap is 9.9 eV [21].

According to the experimental conditions, the complex amplitude A of the light field transmitted through a screen with two holes and through a lens, was set in the form

$$A(x,y,z=0,\tau) = A_0 g_\perp(x,y)\exp\left[i\frac{k(x^2+y^2)}{2f}\right]\exp\left(-\frac{\tau^2}{2\tau_0^2}\right), \quad (3)$$

$$g_\perp(x,y) = \exp\left[-\frac{(x-h/2)^2+y^2}{2r_0^2}\right] + \exp\left[-\frac{(x+h/2)^2+y^2}{2r_0^2}\right]\exp(i\Delta\varphi),$$

where h is the distance between the holes in the screen, r_0 is the hole radius, f is the lens focal length, and $\Delta\varphi$ is the phase shift between the pulses. To perform comparison with the experimental data, the simulation results were used to calculate the integral values of the maximum concentration of free carriers

for the radiation transmission time and the linear densities of the energy flux in different z = const planes:

$$n_e^{(1)}(x,z)=\int n_e^{\max}(x,y,z)\mathrm{d}y,\ n_e^{(2)}(y,z)=\int n_e^{\max}(x,y,z)\mathrm{d}x, \quad (4)$$

$$F^{(1)}(x,z)=\int F(x,y,z)\mathrm{d}y,\ F^{(2)}(x,z)=\int F(x,y,z)\mathrm{d}x. \quad (5)$$

4. Results and discussion

Figure 2 shows photographs of filaments in the beam overlap region, which were recorded by a CCD camera through the lateral face of the sample, as well as continuous-tone patterns for the distributions $F^{(1)}(x, z)$, $F^{(2)}(y, z)$ and $n_e^{(1)}(x, z)$, $n_e^{(2)}(x, z)$, obtained by numerical simulation. We investigated the case of in-phase pulses ($\Delta\varphi$ = 0). The left and right columns correspond to recording in the horizontal (beam propagation) and vertical planes.

In the horizontal plane one can see two crossed narrow filaments with a high fluence and electron density, which form an interference structure in the region of the lens geometric focus (z = 0.5 mm). The maxima of zero and first orders are well distinguished (Fig. 2c). The same data, obtained by observation in the vertical plane, are shown in Fig. 2 on the right. It can clearly be seen that two additional plasma channels are formed outside the plane of initial beam propagation, near the geometric focus of the lens (at a distance of 0.4–0.6 mm from the crystal input face).

To gain more insight into the dynamics of interaction of noncollinear filaments, we constructed 3D isosurfaces of the fluence at a level of 0.15 J cm^{-2} and the electron density at a level of 10^{15} cm^{-3} (Fig. 3). According to these data, one can select the following stages of filament formation in crossed beams. In the first stage (before a significant beam overlap), two independent filaments are formed. A theoretical estimation according to the Marburger formula [22] yields 88 μm for the distance from the crystal input face to the nonlinear focus of the focused beam. The numerical simulation showed a significant increase in the plasma electron density (to 10^{20} cm^{-3}) at a distance of 100 μm. The pulse overlap region exhibits a complex distribution of the fluence F with numerous peaks, whose position indicates that the radiation propagates at large angles with respect to the z axis (up to 10°–12°). Some of them are formed outside the plane of initial beam propagation.

Furthermore, the radiation responsible for these peaks rapidly diffracts, the fluence decreases, and the ionising effect

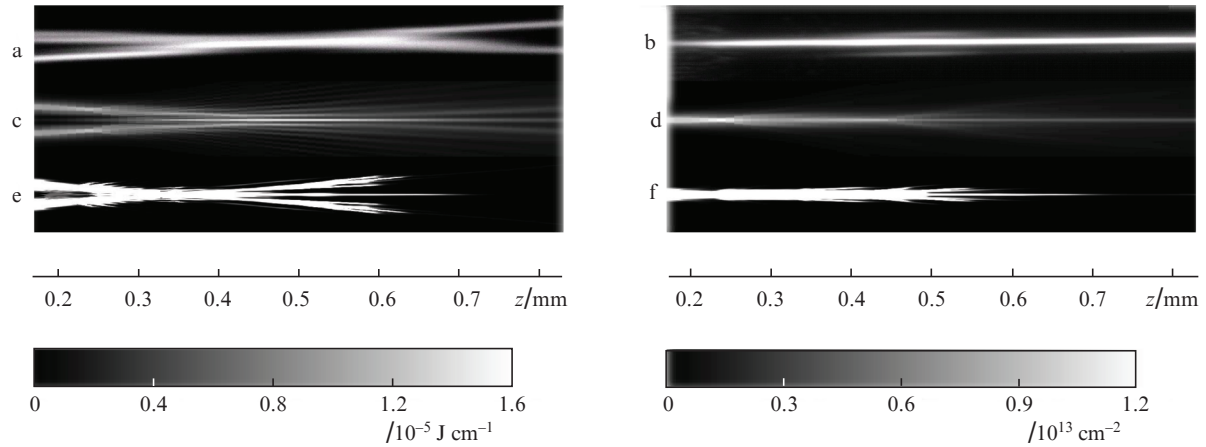

Figure 2. (a, b) Experimental photographs of the filament interaction region in a sapphire sample (side view) and (c–f) the numerical distributions of the linear fluence (c) $F^{(1)}(x, z)$ and (d) $F^{(2)}(y, z)$ and the integral electron density (e) $n_e^{(1)}(x, z)$ and (f) $n_e^{(2)}(y, z)$. The observation was performed in the (a, c, e) horizontal and (b, d, f) vertical planes. The lens focus is located at a distance of 0.5 mm. White colour corresponds to the $F^{(1,2)}$ values exceeding 1.6×10^{-5} J cm^{-1} (c, d) and the $n_e^{(1,2)}$ values exceeding 1.2×10^{13} cm^{-2} (e, f). The diagrams in the bottom row are halftone palettes for the fluence (on the left) and the plasma density (on the right).

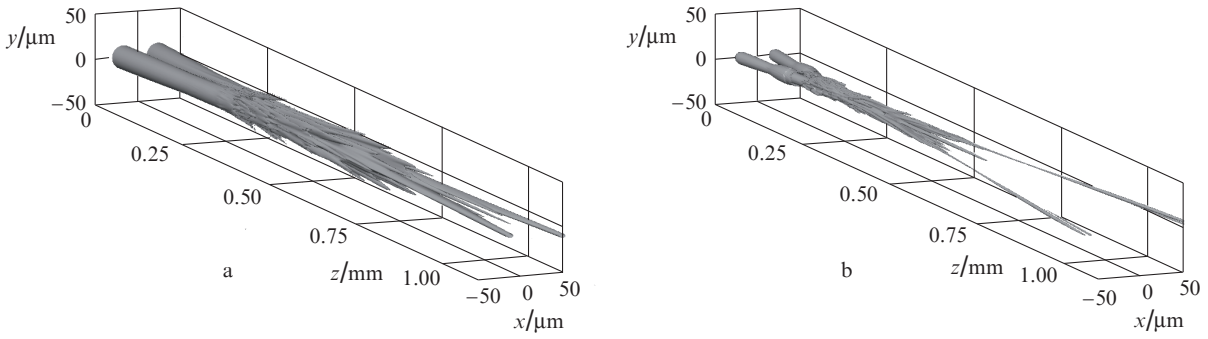

Figure 3. Isosurfaces of (a) the fluence $F(x, y, z)$ at a level of 0.15 J cm^{-2} and (b) the free-electron density $n_e(x, y, z)$ at a level of 10^{15}cm^{-3}. The input peak power of each pulse is 25 MW; the pulses are in-phase.

of radiation becomes insignificant. Behind the waist, the distributions of the fluence and plasma density exhibit three extended filamentary structures, which correspond to two initial beam propagation directions, as well as to the central filament, generated by their interaction.

Note that the maximum values of the linear plasma density

$$n_{ez}^{\max}(z) = \iint n_{e}^{\max}(x,y,z)\mathrm{d}x\mathrm{d}y$$

along the z axis in the case of two in-phase pulses exceeded the corresponding values for a single pulse by 30%–40% and reached 4.5×10^{12} cm^{-1} (at a peak power of each pulse of 25 MW, i.e., $12.5P_{cr}$).

Figure 4 shows the distribution of the fluence in the transverse cross section at $z = 1.5$ mm. Along with the three aforementioned structures, one can see additional 'hot points': traces of energy fluxes in the vertical plane oyz, which is perpendicular to the plane of initial beam propagation.

To characterise quantitatively the propagation directions of energy fluxes, we calculated the fraction of the total radiation energy that was transmitted within the three groups of apertures (*1–3* in Fig. 4). We investigated pairs of in-phase, out-of-phase, and independent pulses. The latter case corresponds to a long time delay between the pulses, at which there was no temporal pulse overlap in the region of the beam waist, and the medium had enough time to completely relax in the time interval between the pulses. The apertures were located in the output plane oxy at a distance of 1 mm behind the lens geometric focus. The diameter of all apertures was 20 μm.

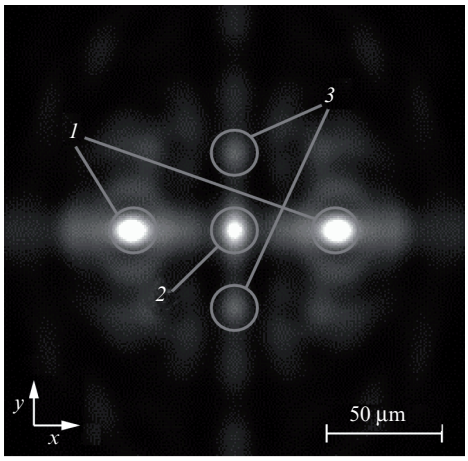

Figure 4. Numerical distribution of the fluence $F(x, y)$ in the transverse beam cross section at a distance of 1.5 mm from the crystal input face. The input peak power of each pulse is 25 MW; the pulses are in-phase. The circles indicate groups of apertures: (*1*) the main apertures, (*2*) the paraxial aperture, and (*3*) the additional apertures.

The apertures of the first (main) group were in the region of 'hot points' of the filaments in the absence of their interaction. In the case of linear propagation the main-group apertures capture approximately half of the pulse energy. The second group included one paraxial aperture, located on the symmetry axis of the system. The apertures of the third group were placed beyond the horizontal plane oxz, above and below the paraxial aperture. If pulses propagate linearly, no more than 1% their energy falls in the second and third groups.

The results of the numerical simulation of the interaction between pulses with input peak powers P_0 ranging from 5 to 25 MW (pulse energies in the range of 0.77–3.8 μJ) are shown in Fig. 5. The energy fractions within the above-mentioned groups of apertures are given for in-phase ($\Delta\varphi = 0$), out-of-phase ($\Delta\varphi = \pi$), and noninteracting pulses.

One can see in Fig. 5a that the energy fraction within the main apertures decreases with increasing pulse energy. For independent pulses the absolute value of the energy transferred by filaments is about 0.25–0.3 μJ; it hardly depends on the input peak power of the pulse. The interaction between pulses in the filamentation regime leads to a decrease in the energy in the main apertures by a factor of about 1.5. As a whole, a considerable part of the pulse energy (up to 90%–95% at $P_0 = 25$ MW) is transferred not through the two main plasma channels but through their energy reservoir, in which additional (weaker) channels can be formed.

The case of out-of-phase pulses is characterised by relatively low energies within the second and third aperture groups (Figs 5b, 5c), which is due to the destructive interference of radiation in the vertical plane oyz. These figures indicate also that, in the case of interacting in-phase pulses, the energy localisation in some areas of the vertical plane is higher than for independent or out-of-phase pulses. This is also

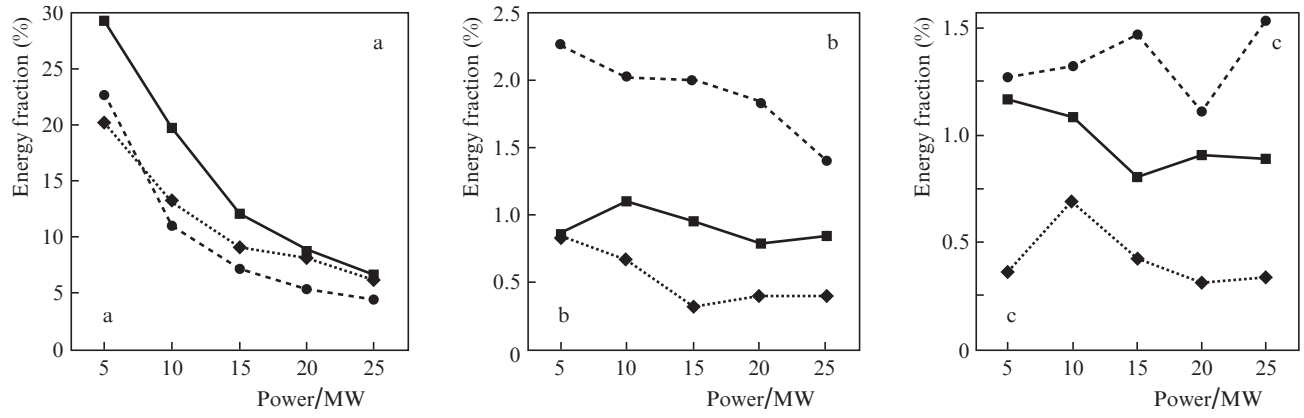

Figure 5. Fraction of the total energy transmitted through the groups of apertures (a) *1*, (b) *2*, and (c) *3* in the case of (circles) in-phase, (diamonds) out-of-phase, and (squares) independent filaments at different peak powers of the initial pulses (results of numerical simulation). The input peak power of each pulse is plotted along the horizontal axis.

caused by the interference effects, as a result of which nonlinear self-action effects are suppressed in the dark interference fringes. Note that the energy transferred by the central plasma channel [paraxial aperture (*2*)] in the geometry under consideration is always lower than the energy in each main aperture (*1*). Therefore, its length is small, and rather soon it disappears (Fig. 3). The length of the additional channels observed outside the horizontal plane at $P_0 = 25$ MW is even smaller.

A comparison of the energies within the aperture groups (*2*) and (*3*) (Figs. 5b, 5c) for interacting pulses with different phase relations shows that, changing the phase shift between these pulses, one can control the fraction and magnitude of energy in the aforementioned apertures in wide limits. Vice versa, the energy transferred through these apertures carries information about the phase relations between the pulses. For in-phase and out-of-phase pulses, the fractions of the total energy transferred through paraxial aperture (*2*) differ by a factor of 3 (2.3% at $\Delta\varphi = 0$ and 0.8% at $\Delta\varphi = \pi$) at a power of 5 MW and by a factor of 6 (2% and 0.32%, respectively) at a power of 15 MW. The fractions of the energy transferred through additional aperture (*3*) differ by a factor of 1.9 at a power of 10 MW (1.3% and 0.7%) and by a factor of 4.5 at a power of 25 MW (1.53% and 0.34%).

5. Conclusions

Upon interaction of two focused crossed coherent laser pulses in a sapphire crystal after the transmission through the waist beam, relatively high fluence (above 0.15 J cm^{-2}) and plasma densities (10^{15} cm^{-3}) were observed in three extended filamentary structures. Two of them (the main filaments) correspond to the initial pulse propagation directions, while the third filament is located at the center on the symmetry axis. The central filament transfers less energy than the main ones and disappears rather soon.

Additional 'hot points' or plasma channels may arise in the plane oriented perpendicularly to the pulse propagation plane. The necessary conditions for their formation is the relatively high input peak pulse power (above $10P_{cr}$,) and the constructive interference of interacting pulses in the paraxial waist region (at $\Delta\varphi = 0$). Changing the phase shift between the pulses, one can change the energies transferred through the central and additional channels (by a factor of 4.5–6). The formation of additional channels can be used for spatial redistribution of radiation with a high fluence.

Acknowledgements. The numerical simulation was performed on the 'Chebyshev' and 'Lomonosov' supercomputers of the Scientific and Research Computing Center, M.V. Lomonosov Moscow State University.

This study was supported by the Russian Foundation for Basic Research (Grant Nos 11-02-90421-Ukr_f_a, 11-02-01100-a, and 11-02-00556-a) and the Ukrainian State Foundation for Basic Research (Project No. F40.2/067).

References

1. Couairon A., Mysyrowicz A. *Phys. Rep.*, **441**, 47 (2007).
2. Kandidov V.P., Shlenov S.A., Kosareva O.G. *Kvantovaya Elektron.*, **39**, 205 (2009) [*Quantum Electron.*, **39**, 205 (2009)].
3. Kandidov V.P., Shlenov S.A. *Glubokoe kanalirovanie i filamentatsiya moshchnogo lazernogo izlucheniya v veshchestve* (Deep Channeling and Filamentation of High-Power Laser Radiation in Matter) (Moscow: Interkontakt Nauka, 2009) Part 2, pp 185–266.
4. Kandidov V.P., Fedorov V.Yu., Tverskoi O.V., Kosareva O.G., Chin S.L. *Kvantovaya Elektron.*, **41**, 382 (2011) [*Quantum Electron.*, **41**, 382 (2011)].
5. Mlejnek M., Wright E.M., Moloney J.V. *Opt. Express*, 4, 223 (1999).
6. Bespalov V.I., Talanov V.I. *Pis'ma Zh. Eksp. Tekh. Fiz.*, **3**, 471 (1966).
7. Bejot P., Bonacina L., Extermann J., Moret M., Wolf J.-P., Ackermann R., et al. *Appl. Phys. Lett.*, **90**, 151106 (2007).
8. Tzortzakis S., Bergé L., Couairon A., Franco M., Prade B., Mysyrowicz A. *Phys. Rev. Lett.*, **86**, 5470 (2001).
9. Bernstein A.C., McCormick M., Dyer G.M., Sanders J.C., Ditmire T. *Phys. Rev. Lett.*, **102**, 123902 (2009).
10. Cai H., Wu J., Lu P., Bai X., et al. *Phys. Rev. A*, **80**, 051802 (2009).
11. Liu Y., Durand M., Chen S., Houard A., Prade B., Forestier B., Mysyrowicz A. *Phys. Rev. Lett.*, **105**, 055003 (2010).
12. Blonskyi I., Kadan V., Shpotyuk O., Korenyuk P., Pavlov I. *Proc. SPIE Int. Soc. Opt. Eng.*, **7993**, 79931C (2010).
13. Xi T.-T., Lu X., Zhang J. *Phys. Rev. Lett.*, **96**, 025003 (2006).
14. Ma Y.-Y., Lu X., Xi T.-T., et al. *Appl. Phys. B*, **93**, 463 (2008).
15. Kandidov V.P., Kosareva O.G., Shlenov S.A., Panov N.A., et al. *Kvantovaya Elektron.*, **35**, 59 (2005) [*Quantum Electron.*, **35**, 59 (2005)].
16. Malitson I.H. *J. Opt. Soc. Am.*, **52**, 1377 (1962).
17. Keldysh L.V. *Zh. Eksp. Tekh. Fiz.*, **47**, 1945 (1964).
18. Shan J., Wang F., Knoesel E., Bonn M., Heinz T.F. *Phys. Rev. Lett.*, **90**, 247401 (2003).
19. Major A., Yoshino F., Nikolakakos I., Aitchison J.S., Smith P.W.E. *Opt. Lett.*, **29**, 602 (2004).
20. Yau T.-W., Lee C.-H., Wang J., in *QELS 2000 Conf.* (San Francisco, California, USA, 2000) paper QWI16.
21. Trager F. *Springer Handbook of Laser and Optics* (New York: Springer, 2007).
22. Marburger J.H. *Progr. Quantum Electron.*, **4**, 35 (1975).